

# DrugScore<sup>RNA</sup>—Knowledge-Based Scoring Function To Predict RNA—Ligand Interactions

Patrick Pfeffer<sup>†</sup> and Holger Gohlke\*

Department of Biological Sciences, Molecular Bioinformatics Group, J.W. Goethe-University,  
Max-von-Laue-Strasse 9, Frankfurt 60438, Germany

Received April 13, 2007

There is growing interest in RNA as a drug target due to its widespread involvement in biological processes. To exploit the power of structure-based drug-design approaches, novel scoring and docking tools need to be developed that can efficiently and reliably predict binding modes and binding affinities of RNA ligands. We report for the first time the development of a knowledge-based scoring function to predict RNA—ligand interactions (DrugScore<sup>RNA</sup>). Based on the formalism of the DrugScore approach, distance-dependent pair potentials are derived from 670 crystallographically determined nucleic acid—ligand and —protein complexes. These potentials display quantitative differences compared to those of DrugScore (derived from protein—ligand complexes) and DrugScore<sup>CSD</sup> (derived from small-molecule crystal data). When used as an objective function for docking 31 RNA—ligand complexes, DrugScore<sup>RNA</sup> generates “good” binding geometries (rmsd (root mean-square deviation) < 2 Å) in 42% of all cases on the first scoring rank. This is an improvement of 44% to 120% when compared to DrugScore, DrugScore<sup>CSD</sup>, and an RNA-adapted AutoDock scoring function. Encouragingly, good docking results are also obtained for a subset of 20 NMR structures not contained in the knowledge-base to derive the potentials. This clearly demonstrates the robustness of the potentials. Binding free energy landscapes generated by DrugScore<sup>RNA</sup> show a pronounced funnel shape in almost 3/4 of all cases, indicating the reduced steepness of the knowledge-based potentials. Docking with DrugScore<sup>RNA</sup> can thus be expected to converge fast to the global minimum. Finally, binding affinities were predicted for 15 RNA—ligand complexes with DrugScore<sup>RNA</sup>. A fair correlation between experimental and computed values is found ( $R_s = 0.61$ ), which suffices to distinguish weak from strong binders, as is required in virtual screening applications. DrugScore<sup>RNA</sup> again shows superior predictive power when compared to DrugScore, DrugScore<sup>CSD</sup>, and an RNA-adapted AutoDock scoring function.

## INTRODUCTION

There is growing interest in RNA as a drug target for antibacterial and antiviral treatment.<sup>1,2</sup> Several reasons account for this. First, a distinct advantage of RNA targets over protein ones is the slower development of drug resistance in a highly conserved RNA motif.<sup>1</sup> Second, in contrast to DNA that solely acts as an “information storage device”, numerous complex functions of RNA molecules have been discovered besides being a passive mediator of genetic information.<sup>3</sup> As such, RNA serves as template (mRNA), ribosome component (rRNA), and activated intermediate (aminoacyl-tRNA) in protein syntheses.<sup>4,5</sup> It also controls gene expression and plays a vital role in the lifecycle of retroviruses such as the HIV-1 virus<sup>6,7</sup> or other pathogenic viruses.<sup>8</sup> Finally, most functions of RNAs require interactions with RNA-binding proteins.<sup>9</sup> Hence, many opportunities to target specific RNA structures or protein—RNA interactions exist. Third, unlike DNA, RNA forms complex three-dimensional structures due to a much larger repertoire of possible base pairings and tertiary structural motifs.<sup>10</sup> The displayed surface topography of these structures in terms of pockets and deep grooves resembles that of protein structures.

In addition, “irregular” RNA motifs such as non-Watson—Crick base pairs, base triples, and bulges provide a functionally rich environment for molecular recognition. Complex recognition strategies can thus be exploited by small-molecules binding to RNA.<sup>9</sup>

The steep increase in functional and structural knowledge of RNA molecules calls for rational, structure-based approaches that lead to the development of novel antibacterial and antiviral drugs. Although successful library screenings for small molecules interfering with RNA functions have been reported,<sup>11–13</sup> the development of such hits into highly specific effectors targeting distinct RNA folds is hardly imaginable without a detailed structural and energetic understanding of RNA recognition.<sup>9</sup> Furthermore, the increasing number of available RNA structures provides the opportunity to apply virtual screening techniques<sup>14</sup> as time- and cost-efficient alternatives to experimental high-throughput screenings.<sup>15–17</sup>

For these structure-based approaches to be successful, appropriate docking and scoring methods have to be developed and evaluated. While the past 25 years have seen great progress in the development of automatic docking tools to predict protein—ligand interactions,<sup>18,19</sup> much less has been achieved in efficiently and accurately modeling RNA—ligand interactions. The current approaches can be divided into three different classes:

\* Corresponding author phone: (+49) 69 798-29411; fax: (+49) 69 798-29527; e-mail: gohlke@bioinformatik.uni-frankfurt.de.

<sup>†</sup> Present address: Department of Pharmaceutical Chemistry, Philipps-University, Marburg, Germany.

**(I) Computationally intense methods** combining docking methods and molecular dynamics simulations. These approaches strive to build models for a small number of RNA–ligand complexes but are too time-consuming for large-scale screening applications.<sup>20–23</sup> These methods will not be further considered here.

**(II) Methods originally developed for protein-based drug design**, which are subsequently applied to RNA. E.g., Kuntz and co-workers used the DOCK program to identify small molecules with binding specificity to the RNA double helix.<sup>24,25</sup> Likewise, Leclerc and Karplus identified favorable RNA binding sites by the MCSS method, thereby making use of nucleic acid parameters from the CHARMM force field.<sup>26</sup> In a virtual screening study, James and co-workers successfully identified acetylpromazine as a lead compound that binds to TAR RNA by a rigid DOCK screen and subsequent flexible docking with ICM.<sup>16</sup> Both methods are well-known for predicting protein–ligand complexes. Interestingly enough, however, for finally ranking the compounds RNA-specific regression-based scoring functions needed to be developed based on very limited structural and energetic knowledge of only 13 RNA–ligand complexes. In a related validation study, Detering and Varani generally concluded that it is possible to use the automated docking tools DOCK and AutoDock developed for proteins to increase the likelihood of discovering molecules in databases that bind to RNA.<sup>27</sup> However, DOCK was successful only in the case of rigid aromatic ligands, whereas it performs poorly with weak-binding ligands and with aminoglycosides. Similarly, AutoDock fails on the complexes for which DOCK performed worse. Very likely, this indicates a misbalance between charged and nonpolar/aromatic interactions in both protein-based scoring functions. Consequently, the highest likelihood of identifying RNA-binding ligands from database screens was only achieved by a successive application of DOCK and AutoDock. Thus, although both studies provide encouraging examples of the current scope of RNA-based virtual screening, at the same time they point to shortcomings in the description of the energetic determinants of RNA–ligand binding.

**(III) Applications Newly Developed for Scoring RNA–Ligand Interactions.** In an attempt to overcome the above-mentioned shortcomings, Morley and Afshar developed a new RNA-specific regression-based scoring function (“RiboDock”).<sup>28</sup> As in the case of the regression-based functions by James and co-workers,<sup>15</sup> however, a limited training and validation set of only 10 RNA–ligand complexes was employed to parametrize the function. Hence, the general applicability and predictive power of this function remains elusive.

The above considerations provided the incentive for developing a knowledge-based scoring function to predict RNA–ligand interactions in this study. To the best of our knowledge, such an approach has not yet been reported. Here, “knowledge-based” refers to deriving energetic information from the statistical analysis of structural parameters of known biomolecules or biomolecular complex structures.<sup>18,29</sup> Knowledge-based scoring functions do not require accurate binding affinity data for training as do regression-based ones. This is clearly an advantage in those cases where only limited data sets are available. Once established, the functions are also easy to rederive on a larger data set. This is advanta-

geous in view of the currently steep increase of structural knowledge about RNA. Knowledge-based functions have been widely applied to score protein–protein,<sup>30</sup> protein–DNA,<sup>31</sup> and protein–ligand interactions.<sup>31–38</sup> In our hands, the DrugScore approach has been proven successful already for scoring<sup>34,39</sup> and predicting<sup>40</sup> protein–ligand complexes. In part, this has been attributed to the implicit, well-balanced consideration of several different types of interactions occurring in protein–ligand complexes, such as polar (including hydrogen bonding), charged, and nonpolar interactions. Obtaining such a delicate balance is also considered crucial for successfully predicting RNA–ligand complexes.<sup>9</sup> Finally, following the idea that like forces should drive the formation of protein–ligand complexes and small-molecule assemblies, we also developed and successfully evaluated knowledge-based potentials from small-molecule crystal data (DrugScore<sup>CSD</sup>) recently.<sup>41</sup> Transferring this idea to the problem of sparse data in the case of RNA–ligand complexes, we anticipated that valuable information for scoring RNA–ligand complexes can additionally be derived from RNA–protein and DNA–protein complexes.

## METHODS

### Distance-Dependent Pair-Potentials and Binding Score.

For deriving the distance-dependent pair-potentials of the new scoring function DrugScore<sup>RNA</sup>, the same formalism is applied as already described for the DrugScore scoring function for protein–ligand complexes.<sup>34</sup> Following an inverse Boltzmann and modified Sippl approach,<sup>42</sup> specific interactions  $\Delta W_{T(l),T(n)}(r)$  between ligand atom *l* of type T(*l*) and nucleic acid atom *n* of type T(*n*), separated by a distance *r*, can be obtained from the normalized radial pair-distribution function  $g_{T(l),T(n)}(r)$  and the normalized mean radial pair distribution function  $g(r)$ :

$$\Delta W_{T(l),T(n)}(r) = -\ln \frac{g_{T(l),T(n)}(r)}{g(r)} \quad (1)$$

$g_{T(l),T(n)}(r)$  is computed from occurrence frequencies  $N_{T(l),T(n)}(r)$  of atom pairs with types T(*l*) and T(*n*) according to

$$g_{T(l),T(n)}(r) = \frac{N_{T(l),T(n)}(r)/4\pi r^2 dr}{\sum_r (N_{T(l),T(n)}(r)/4\pi r^2 dr)} \quad (2)$$

$4\pi r^2 dr$  is a scaling factor that takes into account the volume of a shell with radius *r* and thickness *dr*. DrugScore<sup>RNA</sup> pair potentials consider atom–atom interactions within a distance range from 1 to 6 Å. The upper limit of 6 Å ensures that only direct RNA–ligand interactions are considered but no bridging water molecules. Furthermore, considering only short-range interactions renders the use of volume correction factors that account for occupied volume around a considered atom<sup>32</sup> unnecessary as these markedly differ only over large distance ranges.<sup>38</sup> The bin size *dr* is set to 0.1 Å.

Choosing a proper reference state is crucial to the predictive power of knowledge-based scoring functions.<sup>43,44</sup> In our case, the reference state  $g(r)$  mimics a compact RNA–ligand configuration with nonspecific interactions. Thus, the reference state removes “zero-interaction” contacts from the

distributions such that net potentials representing only specific interactions are obtained. All other parameters were chosen as described in ref 34.

$$g(r) = \frac{\sum_{T(l)} \sum_{T(n)} g_{T(l),T(n)}(r)}{||T(l)|| \cdot ||T(n)||} \quad (3)$$

The “binding score” for a complex of an RNA molecule  $N$  and a ligand  $L$  is calculated as the sum of all occurring atom–atom interactions.

$$\Delta W = \sum_{l \in L} \sum_{n \in N} \Delta W_{T(l),T(n)}(r) \quad (4)$$

**Knowledge Base for Deriving Pair Potentials.** RNA-specific distance-dependent pair potentials are derived from crystallographically determined nucleic acid–ligand and –protein complexes using an in-house MySQL database that contains structural information of all PDB entries (Schmidt, E.; Derksen, S.; Gohlke, H. unpublished results). Initially, only 50 crystallographically determined RNA–ligand complexes were considered, with ligands containing between 6 and 50 non-hydrogen atoms. Metal ions were included as part of the binding site to reproduce the ligand’s environment as experimentally determined. However, only statistically insignificant distribution functions could be derived. To extend the knowledge base, NMR-derived RNA–ligand complexes were considered in addition. This did not yield potentials of satisfying predictive power, presumably, due to the lower resolution of the experimental data. NMR-derived structures were thus not considered any further. Instead, we resorted to also take into account DNA–ligand complexes, where similar interactions as in the RNA case should occur. Finally, to even further strengthen our knowledge base, we decided to also include nucleic acid–protein and –peptide complexes: In almost half of the PDB entries containing nucleic acids, proteins or peptide chains are cocrystallized. In all cases, the complexes had been resolved to at least 2.5 Å. In total, 670 nucleic acid complexes were used to derive the distance-dependent pair potentials of DrugScore<sup>RNA</sup>. PDB codes of all complexes used for deriving the potentials are listed in Table S1 in the Supporting Information. Potentials were derived for all DrugScore standard atom types, which are similar to the Sybyl atom-type notation.<sup>45</sup> See ref 34 for further details.

**Validating the DrugScore<sup>RNA</sup> Potentials.** The predictive power of the DrugScore<sup>RNA</sup> potentials was assessed in terms of their ability to reconstruct nativelike RNA–ligand complex geometries in self-docking experiments, the funnel-shapeness of the resulting energy landscapes, and the correlation between experimentally determined binding free energies and calculated binding scores (eq 4).

The data set used for docking consists of 31 noncovalent RNA–ligand complexes where the ligands have druglike characteristics (Table S2 in the Supporting Information). This data set is by far the largest data set used up to now for validating a RNA–ligand scoring function. It also comprises all those complexes that have been used in the studies of Detering et al.<sup>27</sup> (14 complexes), Morley et al.<sup>28</sup> (10 complexes), and Filikov et al.<sup>15</sup> (5 complexes) for validation

purposes. Hence, results obtained with DrugScore<sup>RNA</sup> for subsets of these complexes can be directly compared to these studies.

The AutoDock<sup>46</sup> program generates complex geometries by directly optimizing an energy or scoring function. It allows supplying external scoring functions by the user.<sup>40,47</sup> Accordingly, AutoDock was selected to test the performance of DrugScore<sup>RNA</sup> in guiding docking searches, with energy grids computed from DrugScore<sup>RNA</sup> potentials. Likewise, energy grids were computed from DrugScore and DrugScore<sup>CSD</sup> for reasons of comparison. See ref 40 for further details. Standard AutoDock potentials were used for considering intramolecular ligand energies during the docking; however, the final ranking is determined only by intermolecular energies. In the recent version 3.0.5 of AutoDock, the Lamarckian genetic algorithm (LGA) has been used for exploring ligand space. LGA runs were performed using standard parameters provided by AutoDock, with 10<sup>6</sup> energy evaluations performed in 100 independent runs using a population size of 100 individuals.

The RNA structures were held rigid during the docking, and no water molecules were taken into account. As an interesting alternative, Moitessier et al.<sup>48</sup> recently reported docking to hydrated and flexible RNA. However, this approach requires extensive experimental information (i.e., cocrystal structures of several ligands bound to the same target) and was tested only for aminoglycosides bound to the ribosomal A-site RNA. Thus, as also stated by these authors, the transferability of the method to other classes of molecules still needs to be assessed.<sup>48</sup>

**Data Set Preparation for Docking Using the AutoDock Energy Function.** A subset of the validation data set was used to assess the predictive power of the regression-based energy-function of AutoDock. This scoring function was modified according to Detering et al.,<sup>27</sup> namely, solvation parameters were added for RNA atoms, and nitrogen atoms accepting and not accepting hydrogen bonds were separately defined for the grid map calculation. After separating RNA and ligand molecules, protons were added to the crystal geometries using standard geometrical parameters. Partial charges were assigned to the RNA using the Cornell et al.<sup>49</sup> force field except for P atoms, for which increased charges were applied according to Detering et al.<sup>27</sup>

**Ligand Preparation.** For all scoring functions tested (DrugScore, DrugScore<sup>CSD</sup>, DrugScore<sup>RNA</sup>, and AutoDock) the ligands were prepared in the same way using the Autotors utility from the AutoDock suite of programs to assign rotatable bonds. In addition, for AutoDock, Gasteiger–Marsili atomic charges were assigned<sup>50</sup> as implemented in the program Antechamber from the Amber8 suite of programs.<sup>51</sup>

## RESULTS AND DISCUSSION

Knowledge-based approaches have been widely applied for analyzing protein–protein,<sup>30</sup> protein–DNA,<sup>31</sup> and protein–ligand interactions.<sup>31–38</sup> DrugScore<sup>RNA</sup> is, to the best of our knowledge, the first knowledge-based approach to score RNA–ligand complexes. So far, it has been considered rather unlikely to obtain statistically significant potentials due to the small number of experimentally determined RNA–ligand complexes. In fact, we could only derive statistically insignificant distribution functions based on such data.

Therefore, we decided to also include DNA–ligand complexes as well as RNA/DNA–protein complexes in our knowledge base. We anticipated that atom–atom interactions in these systems are similar enough to those in RNA–ligand systems. As with all empirical approaches, such a procedure can only be validated by the predictive power and ability to reproduce experimental data.

In the following, we will first compare nucleic acids-derived knowledge-based potentials (DrugScore<sup>RNA</sup>) to the ones of DrugScore<sup>34</sup> and DrugScore<sup>CSD</sup>.<sup>41</sup> We will then evaluate their predictive power with respect to recognize near-native geometries of RNA–ligand complexes, construct funnel-shaped binding (free) energy surfaces, and predict binding affinities.

**Characteristics of Nucleic Acids-Based Pair Distributions and Potentials.** The significance of knowledge-based pair potentials increases with the amount of structural data from which pair distribution functions (eq 2) are derived. Previous experiences indicate that at least 500 interactions (i.e., about 10 interactions per distance bin) are required per atom–atom pair to obtain statistically significant potentials.<sup>34,41</sup> In that sense, the knowledge base is considerably increased if the combined nucleic acid–ligand/protein complexes are used instead of only RNA–ligand complexes. E.g., whereas in the latter case only 699 C.3-C.3 and 78 O.2-O.3 interactions would have been considered, these numbers increased to 173 961 and 47 406, respectively, in the case of the comprehensive data set. Yet, the occurrence frequencies of pair contacts are still lower in many cases for DrugScore<sup>RNA</sup> compared to DrugScore or DrugScore<sup>CSD</sup>. Conversely, for interactions involving aromatic nitrogen, phosphorus, or oxygen, much higher populated pair distributions are obtained. Considering the different chemical compositions of nucleic acids, proteins, and small molecules, this is not unexpected. These findings may already provide a hint as to why DrugScore<sup>RNA</sup> shows superior predictive power in the case of RNA–ligand complexes compared to DrugScore or DrugScore<sup>CSD</sup> (see below).

Figures 1–3 show examples of pair potentials for interactions between charged atoms of types N.3 and O. co2, polar interactions between O.3 and O.3, and aromatic interactions between C. ar and C. ar. At a first glance, the three potentials show qualitatively similar shapes and relative positions of the minima. Yet, quantitative differences in the potentials are obvious that can be explained by the characteristics of the knowledge base used for the potential derivation. As for all three potentials at least 795 (in the case of N.3-O. co2), 7106 (O.3-O.3), and 16 692 (C. ar-C. ar) pair contacts were available in the databases, the observed differences can be considered significant. It has already been noted<sup>41</sup> that pair distributions derived from small-molecule crystal structures show the most pronounced first and second maxima. This is due to the fact that the resolution of such crystal structures is much higher, and, accordingly, the uncertainties in atomic coordinates are lower. In contrast, PDB-derived pair distributions are much more blurred. Accordingly, minima in the pair potentials have in general a narrower shape in the DrugScore<sup>CSD</sup> case compared to DrugScore<sup>RNA</sup> and DrugScore.

Pronounced differences are also visible with respect to the depths of minima: whereas DrugScore and DrugScore<sup>CSD</sup> show rather similar well depths, this is true only in the case

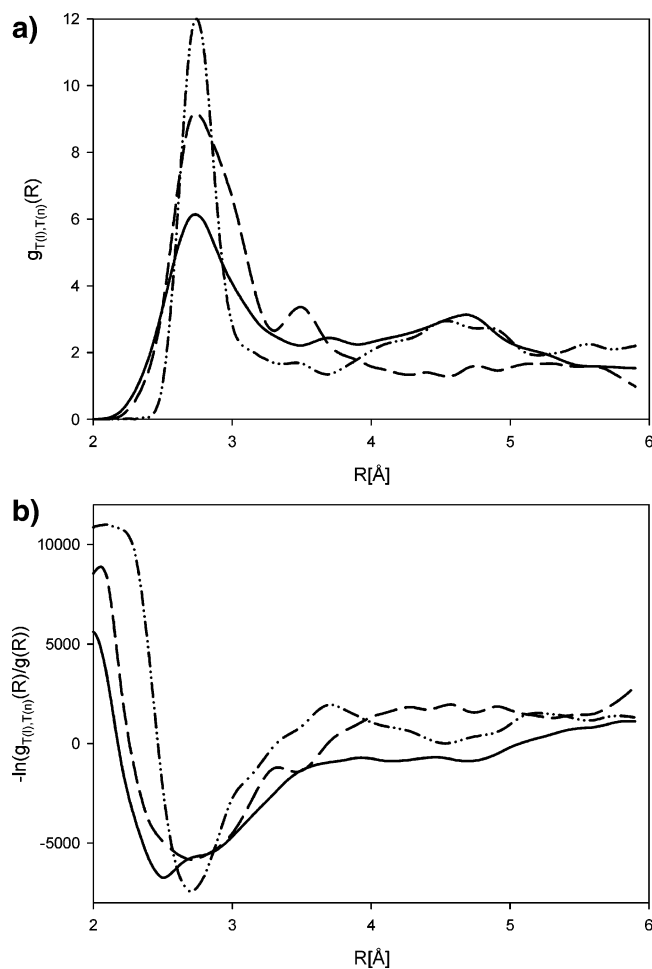


**Figure 1.** Distance-dependent pair distribution (a) and pair potential (b) for charged interactions between atoms of types N.3 and O.co2: DrugScore<sup>RNA</sup> (straight line), DrugScore (dashed), and DrugScore<sup>CSD</sup> (dashed-dotted).

of the N.3-O. co2 interaction for DrugScore<sup>RNA</sup> (Figure 1). In contrast, O.3-O.3 interactions are much less favorable in the DrugScore<sup>RNA</sup> case ( $\Delta W \approx -2000$ ) compared to DrugScore and DrugScore<sup>CSD</sup> ( $\Delta W \approx -4000$ ) (Figure 2). Conversely, C. ar-C. ar interactions are more favorable in the former case ( $\Delta W \approx -2500$  (DrugScore<sup>RNA</sup>);  $-500$  (DrugScore, DrugScore<sup>CSD</sup>)) (Figure 3). These findings reflect the fact that polar interactions between ligands and sugar moieties are less frequent in nucleic acids (and, hence, are interactions to atoms of type O.3), whereas (stacking) interactions between ligands and bases are a hallmark of molecular recognition involving RNA and DNA.<sup>1,9</sup>

**Predicting Near-Native Ligand Geometries.** For 31 RNA–ligand complexes, near-native ligand geometries were predicted with AutoDock, using potential fields of DrugScore<sup>RNA</sup>, DrugScore, DrugScore<sup>CSD</sup>, and an RNA-adapted AutoDock scoring function<sup>27</sup> as objective functions. We note that this is the largest validation data set of RNA–ligand complexes used to date. The results are summarized in Table 1, and details of the docking results are listed in Table S3 in the Supporting Information.

Encouragingly, using DrugScore<sup>RNA</sup>, in 42% of the cases a “good” solution (rmsd (root mean-square deviation)  $\leq 2.0$  Å to the native structure) is found on the first scoring rank. Compared to the results of the other three functions, this is an improvement of 44% in the case of DrugScore<sup>CSD</sup>,

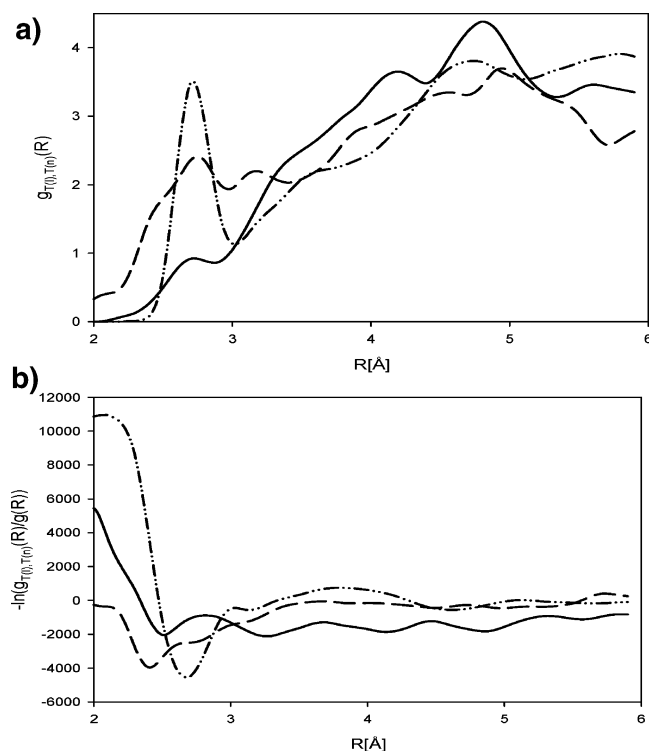


**Figure 2.** Distance-dependent pair distribution (a) and pair potential (b) for the polar interaction between atoms of types O.3 and O.3: DrugScore<sup>RNA</sup> (straight line), DrugScore (dashed), and DrugScore<sup>CSD</sup> (dashed-dotted).

62% in the case of AutoDock, and 120% in the case of DrugScore. It is not unexpected that DrugScore (which has been derived using solely protein–ligand data) performs worst, which demonstrates a database dependence of the statistical potentials.<sup>52</sup> In turn, it is intriguing to note that DrugScore<sup>CSD</sup> performs slightly better than the RNA-adapted AutoDock scoring function. Given that DrugScore<sup>CSD</sup> also shows convincing predictive power in the case of protein–ligand complexes,<sup>41</sup> information derived from small-molecule crystals is apparently general enough to also score intermolecular interactions in systems that are only distantly related. DrugScore<sup>RNA</sup> also performs best if docking solutions with smaller rmsd thresholds (1.0 Å or 1.5 Å) are considered. Still, the results fall short when compared to protein–ligand docking where scoring functions achieve success rates between 70%<sup>41</sup> and 90%<sup>53</sup> in recognizing a good docking solution on the first rank. Two reasons can be anticipated for this: (i) the amount of data used to derive DrugScore<sup>RNA</sup> may still not be sufficient to yield a robust scoring function and (ii) predicting RNA–ligand geometries may be more difficult due to the prevalence of charged and aromatic interactions, which requires a better balance of the energy contributions.

An example for the latter case is given by a high affinity aptamer–theophylline complex (PDB code 1eht)<sup>54</sup> (Figure 6a). In the native structure, the ligand is bound to the well-ordered pocket by stacking interactions to C8 and A7, whereas only a weak hydrogen bond to U24 or even repulsive interactions between the carbonyl atoms and the RNA backbone can be observed. Thus, there are no strong directed interactions that lock in the ligand, and the observed directed pose appears to result from a combination of (subtle) energy contributions. DrugScore<sup>RNA</sup> instead scores best a solution

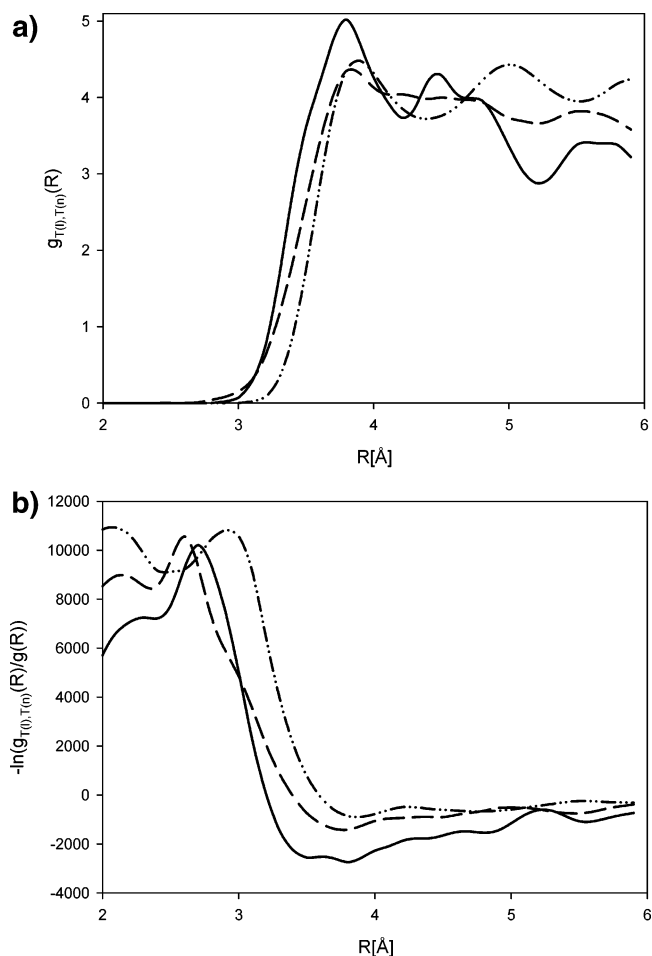


**Figure 3.** Distance-dependent pair distribution (a) and pair potential (b) for the aromatic interaction between atoms of types C.ar and C.ar: DrugScore<sup>RNA</sup> (straight line), DrugScore (dashed), and DrugScore<sup>CSD</sup> (dashed-dotted).

**Table 1.** Docking Results for 31 RNA–Ligand Complexes<sup>a</sup>

	proportion of complexes exhibiting rmsd		
	<1.00 Å	<1.50 Å	<2.00 Å
DrugScore <sup>RNA</sup> <sup>b</sup>	16.13	29.03	51.61
DrugScore <sup>RNA</sup> <sup>c</sup>	9.68	19.35	41.94
DrugScore <sup>b</sup>	19.35	25.81	48.39
DrugScore <sup>c</sup>	9.68	12.90	19.35
DrugScore <sup>CSD</sup> <sup>b</sup>	12.90	38.71	54.84
DrugScore <sup>CSD</sup> <sup>c</sup>	6.45	9.68	29.03
Autodock <sup>b</sup>	22.58	45.16	70.97
Autodock <sup>c</sup>	6.45	12.90	25.81

<sup>a</sup> The percentage of complexes found below a given rmsd from the native structure is shown. <sup>b</sup> Proportion of complexes for which at least one docking solution with the given rmsd was computed irrespective of the scoring rank. <sup>c</sup> Only the docking solution found on the first scoring rank is considered.

where the ligand is flipped by 180°. Given that the stacking interaction remains very similar and considering the formation of strong hydrogen bonds between O2 of theophylline and N3 of U24 as well as O6 of theophylline and N4 of C22, this pose intuitively seems as plausible as the native one.

At this point it is interesting to contrast the performance of DrugScore<sup>RNA</sup> for aptamer complexes (such as the theophyllin complex 1eht), which were evolved to fit to a ligand, to those RNA targets for which small molecules have

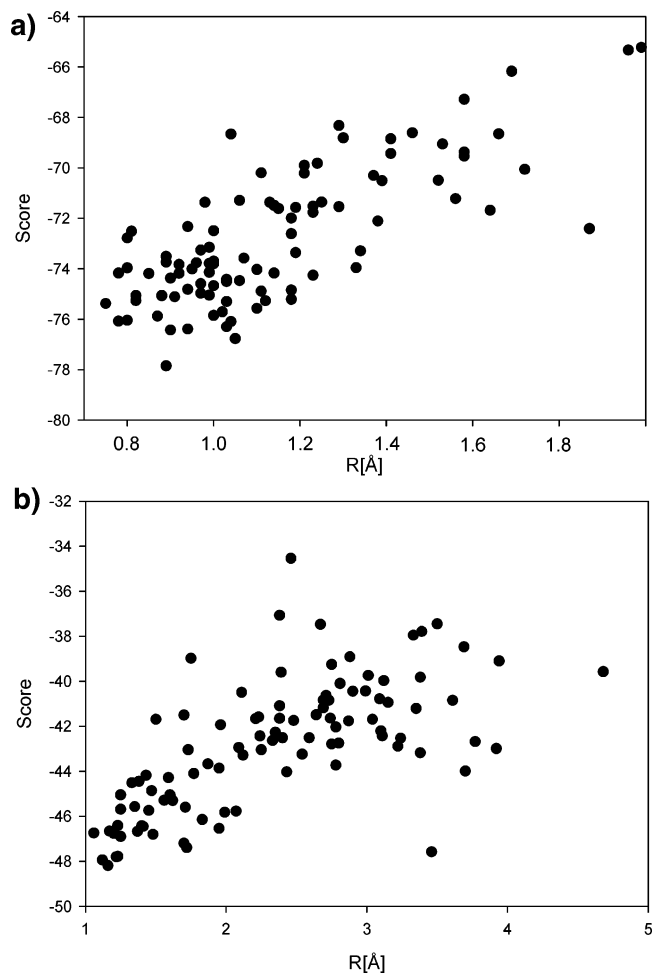


**Figure 4.** Computed scoring values of docking solutions using DrugScore<sup>RNA</sup> as a function of the rmsd from the native structure: Ipbr (panel a) and Ifyp (panel b). Small rmsd values denote near-native-like RNA–ligand configurations.

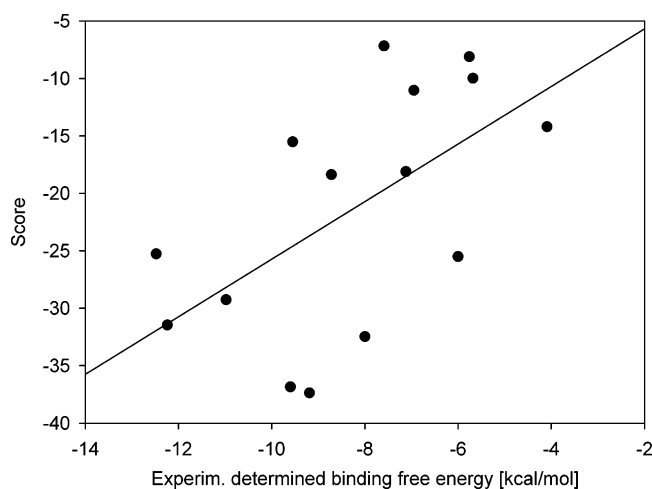


**Figure 5.** Correlation between experimentally determined binding free energies and scores calculated by DrugScore<sup>RNA</sup> of 15 RNA–ligand complexes. The correlation coefficient is  $R_s = 0.61$ .

evolved as ligands.<sup>55</sup> An example for the latter case is given by the ribosomal decoding site in complex with gentamicin (PDB code 1byj)<sup>56</sup> (Figure 6b). Here, complex formation mainly occurs by polar interactions between amino and hydroxyl groups of the ligand and phosphate and polar base atoms of the RNA, whereas only the alicyclic purposamine moiety of gentamicin stacks above the base moiety of G1491.

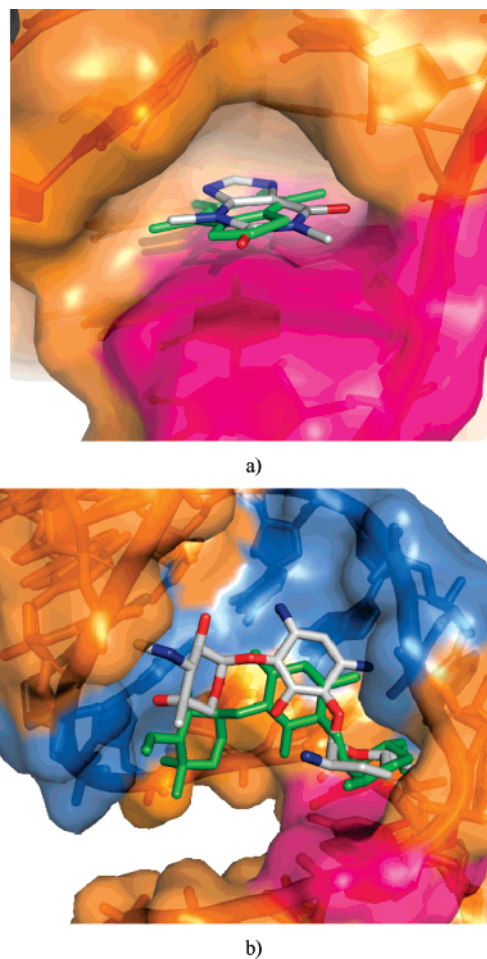


**Figure 6.** (a) Aptamer–theophylline complex (PDB code 1eht). The two base-paired nucleotides C8 and A7 that form a platform in the well-formed binding pocket above which the theophyllin stacks are depicted in magenta. (b) Ribosomal A site–gentamicin complex (PDB code 1byj). G1491 above which the purposamine moiety stacks is depicted in magenta; RNA residues that are involved in polar interactions are depicted in blue. In both cases, the experimental ligand pose is given in light gray, and the docking solution ranked first by DrugScore<sup>RNA</sup> is depicted in green.

Encouragingly, the best scored docking solution deviates by less than 2 Å, with the garosamine moiety deviating the most. This indicates that DrugScore<sup>RNA</sup> properly scores the network of polar interactions in this case, despite the rather open binding site compared to the aptamer–theophylline case.

Overall, of the 31 RNA–ligand complexes of our validation data set, 13 are formed by aptamers, whereas 18 involve natural RNA targets. The mean rmsd of a docking solution found on rank one is  $2.1 \pm 0.9$  Å for the former class and  $2.8 \pm 1.5$  Å for the latter. Likewise, in the aptamer case a “good” docking solution is found in 54% of the cases on the first rank, whereas a “good” docking solution is found only in 33% of the cases of RNA targets from biological sources. Thus, DrugScore<sup>RNA</sup> performs better for aptamer targets, although the limited number of samples precludes a definite answer. This finding is not unexpected in view of the known differences in the characteristics of binding pockets of these two target classes: as aptamers bind their ligands by adaptive recognition, the intricate encapsulation of large parts of the ligand by the nucleic acid is the basis for specific recognition of the cognate ligand.<sup>55</sup> In turn, natural RNA was optimized with respect to multiple aspects

**Table 2.** Comparison of DrugScore<sup>RNA</sup> with Three Other RNA–Ligand Scoring Functions<sup>a</sup>

	Filikov et al. <sup>b</sup>	Detering et al. <sup>c</sup>	Ribodock <sup>d</sup>
Respective function	0.00	42.85	50.00
DrugScore <sup>RNA</sup>	80.00	71.43	90.00

<sup>a</sup> The percentage of complexes is given for which a docking solution with rmsd < 2.0 Å from the native complex was found on the first scoring rank. For all comparisons only the complexes used by the respective scoring functions are also considered by DrugScore<sup>RNA</sup>.  
<sup>b</sup> Docking results for 5 RNA–ligand complexes.<sup>15</sup> <sup>c</sup> Docking results for 14 RNA–ligand complexes.<sup>27</sup> <sup>d</sup> Docking results for 10 RNA–ligand complexes.<sup>28</sup>

of their cellular functions, trading off specificity in ligand binding for additional functions. The finding also parallels results from protein–ligand docking. Here, the highest degree of docking accuracy is found for complexes with buried binding pockets, too, because the best pose for a given ligand is more unequivocally defined in a sterically constrained site.<sup>57</sup>

When considering the percentage of docking solutions for which a good solution has been generated in 100 different docking runs *irrespective of the scoring rank*, the AutoDock scoring function outperforms the knowledge-based potentials (71% vs 48–55%). However, in only 36% (=26/71%) of these cases a good docking solution can also be recognized by the AutoDock scoring function on the first rank. In contrast, this is true in 81% (=42/52%) of such cases for DrugScore<sup>RNA</sup>. Thus, DrugScore<sup>RNA</sup> displays a significantly higher *relative* success rate of recognizing good solutions, in addition to showing a much higher *absolute* success rate of generating good docking solutions on the first rank (as discussed above). This also holds compared to DrugScore<sup>CSD</sup> (53%) and DrugScore (40%). This finding thus suggests a two-step approach to combine the benefit of both functions in the future: First, the RNA-modified AutoDock scoring function is used for generating ligand geometries. Subsequently, the poses are scored in a postprocessing step by DrugScore<sup>RNA</sup>. Analogous approaches have been described in the field of protein–ligand docking.<sup>34,41</sup> We have not pursued such an approach in this study.

Furthermore, we compared our docking results to those described by Detering et al.,<sup>27</sup> Morley et al.,<sup>28</sup> and Filikov et al.<sup>15</sup> (Table 2). In each case, only those complexes were analyzed that were also part of the data set used in the respective study. In all cases, DrugScore<sup>RNA</sup> performed superior to the other approaches: the success rate of finding a good docking solution on the first rank is at least 30% higher. Although these comparisons are based on rather small data sets (e.g., only five complexes in the case of Filikov et al.<sup>15</sup>), which limits the statistical significance, we consider this result a convincing demonstration of the predictive power of our scoring function.

Twenty out of the 31 complexes in the validation data set are NMR structures and, thus, have not been included in the knowledge-base used to derive DrugScore<sup>RNA</sup>. These complexes can be considered an “external test set” because their docking is not influenced by any training effects. With DrugScore<sup>RNA</sup>, a good docking solution is predicted on the first rank for 60% of these complexes, which is even higher than in the case of the total data set. In our view, this clearly demonstrates the robustness of the derived potentials.

**Table 3.** Correlation between rmsd Values and Docking Scores

	cumulative occurrence of $R_S^a$			
	≥0.20	≥0.40	≥0.60	≥0.80
DrugScore <sup>RNA</sup>	74	48	23	0
DrugScore	61	32	6	6
DrugScore <sup>CSD</sup>	61	23	13	3
AutoDock	55	32	16	3

<sup>a</sup> In %.

**Analysis of Binding Energy Landscapes.** The reduced steepness of knowledge-based potentials compared to force-field-based or empirical scoring functions has been recognized as an advantage in docking,<sup>53</sup> as the former functions are more robust to small changes in a receptor conformation and lead to less rugged binding energy surfaces. Along these lines, Wang et al.<sup>58</sup> have analyzed the abilities of scoring functions to construct funnel-shaped (free) energy surfaces of protein–ligand complexation.<sup>59–61</sup> This is based on the reasoning that an ideal scoring function not only should recognize near-native docking solutions reliably but also should produce an energy surface that is smooth as to not impair the efficiency of conformational sampling.

The Spearman correlation coefficient  $R_S$ <sup>62</sup> was used as a quantitative measure to determine the correlation between the rmsd value and the binding scores of docking solutions by these authors. Although not sufficient to comprehensively define the funnel-shapeness of the energy surface due to the high-dimensional character of the latter, such a correlation was assumed to be at least necessary for a funnel to exist. Here, we adopt the same measure. Cumulative occurrences of  $R_S$  values calculated for all docking solutions of the RNA–ligand complexes are given in Table 3. Figure 4 exemplarily shows binding score vs rmsd plots of the complexes 1pbr ( $R_S = 0.68$ ) and 1fyp ( $R_S = 0.64$ ).

DrugScore<sup>RNA</sup> yields  $R_S$  values between 0.60 and 0.80 (no significant numbers are obtained for higher  $R_S$  values) for 23 out of 31 cases (74%), whereas the second best function AutoDock only provides these funnel-like shapes in 52% of the cases. Dockings applying DrugScore<sup>RNA</sup> can thus be expected to converge faster to the global minimum than if the other knowledge-based approaches or the AutoDock scoring function is used. Not unexpectedly, this trend parallels the prediction of good docking solutions on the first rank (see above), where DrugScore<sup>RNA</sup> also outperforms the other approaches.

**Binding Affinity Estimation.** Finally, we evaluated the capability of DrugScore<sup>RNA</sup> to estimate binding affinities. Correctly ranking different ligands with respect to their binding affinity is of utmost importance for virtual screening and de novo design. Yet, reliably estimating binding affinities is still a major challenge in structure-based drug design.

Figure 5 depicts DrugScore<sup>RNA</sup> scores of the best ranked docking solutions vs experimental binding free energies for 15 RNA–ligand complexes (see also Table S4 in the Supporting Information). We consider this a more stringent test than estimating binding affinities for crystallographically determined RNA–ligand configurations. As reliable affinity predictions can only be expected for near-native ligand poses, in our case successful predictions will also depend on the capability of DrugScore<sup>RNA</sup> to identify good docking solutions. At the same time, our test mimics a “real-life scenario”

in which usually no experimental structure is available for the affinity prediction.

A fair correlation between experimental and predicted values is found, as is corroborated by a Spearman rank correlation coefficient of  $R_S = 0.61$ . No over- or underprediction of particular ligand classes is observed, and the prediction accuracy is similar over the whole range of experimental binding free energies. The prediction accuracy is not yet sufficient for ligand optimization. However, the demonstrated predictive power suffices to distinguish weak from stronger binders, as is required in virtual screening applications. When compared to the other three scoring functions (DrugScore:  $R_S = 0.45$ ; DrugScore<sup>CSD</sup>:  $R_S = 0.47$ ; AutoDock:  $R_S = 0.43$ ), DrugScore<sup>RNA</sup> clearly shows a superior predictive power for estimating binding affinities.

It has been noted repeatedly in the case of protein–ligand complexes that binding affinities scale rather well with the molecular weight of the ligands.<sup>41,53</sup> In fact, affinity predictions purely based on the ligand's molecular weight have given better results than many scoring functions.<sup>41</sup> This does not hold for the RNA–ligand complexes investigated here: the correlation between the ligand mass and the affinities yields an  $R_S$  of 0.29. Compared to the DrugScore<sup>RNA</sup> predictions, this correlation is much weaker.

## CONCLUSION

Binding of small-molecules to RNA is governed by a delicate balance of electrostatic forces and stacking interactions.<sup>9</sup> Further contributions may arise from water-mediated contacts and binding to metal ions. This broad spectrum of enthalpic and entropic determinants of molecular recognition involving RNA requires a well-balanced consideration of several different types of interactions when it comes to scoring RNA–ligand complexes.<sup>9</sup> Knowledge-based approaches can provide such a delicate balance, if the database they are derived from is sufficiently large and appropriately represents the systems of interest.

Encouraged by our previous experiences in the field of protein–ligand complexes in this regard, here, we have developed the first knowledge-based scoring function to predict RNA–ligand interactions, DrugScore<sup>RNA</sup>. Based on the concept and formalism of DrugScore, the novel function was derived from 670 crystallographically determined nucleic acid–ligand and nucleic acid–protein complexes. That way, the problem of sparse data in the case of RNA–ligand complexes is overcome such that statistically significant potentials are obtained for most of the pair interactions considered. These pair interactions show characteristic atom–atom interactions for RNA–ligand systems that are quantitatively different from protein–ligand- and small-molecule-derived potentials.

When applied as an objective function in docking to a data set of 31 RNA–ligand complexes, the predictive power of DrugScore<sup>RNA</sup> is demonstrated. We note that this data set is the largest one used for such a validation to date. DrugScore<sup>RNA</sup> succeeds in predicting good docking solutions on the first scoring rank in 42% of the cases and outperforms DrugScore, DrugScore<sup>CSD</sup>, and a modified AutoDock scoring function. When compared to three other RNA–ligand scoring functions for smaller subsets of the test data, DrugScore<sup>RNA</sup> also shows superior performance.

As one of the reasons for DrugScore<sup>RNA</sup>'s success in docking the fact may be considered that the binding (free) energy landscape obtained by these potentials is more funnel-shaped than in the case of the other knowledge-based scoring functions or AutoDock. This is expected to lead to a faster convergence of the dockings to a global minimum or, phrased differently, a reduced likelihood for the configurational search to get stuck in a local minimum.

Finally, binding scores predicted by DrugScore<sup>RNA</sup> show a fair correlation ( $R_S = 0.61$ ) with experimental binding free energies. We stress that only docking solutions found on the first scoring rank were used for the affinity predictions but no experimental structures. This procedure complies with a “real-life scenario” for virtual screening. When compared to the other knowledge-based scoring functions or the modified AutoDock scoring function, DrugScore<sup>RNA</sup> clearly performs best. Yet, the prediction accuracy is still not sufficient for ligand optimization, and more work is needed in this area.

Nevertheless, we consider the success of DrugScore<sup>RNA</sup> convincing, and it is our hope that DrugScore<sup>RNA</sup> will become a valuable tool for the structure-based development of RNA ligands.

## ACKNOWLEDGMENT

This work was supported by the Sonderforschungsbereich (SFB) 579 of the Deutsche Forschungsgemeinschaft and startup funds from J.W. Goethe-University, Frankfurt. We are grateful to Simone Fulle, Domingo González Ruiz, and Sebastian Radestock (University of Frankfurt) for critically reading the manuscript. The DrugScore<sup>RNA</sup> potentials are available from H.G. upon request.

**Supporting Information Available:** Four tables with details about PDB complexes used to derive DrugScore<sup>RNA</sup>, the test data set, docking results, and binding affinity predictions. This material is available free of charge via the Internet at <http://pubs.acs.org>.

## REFERENCES AND NOTES

- (1) Gallego, J.; Varani, G. Targeting RNA with small-molecule drugs: therapeutic promise and chemical challenges. *Acc. Chem. Res.* **2001**, *34*, 836–843.
- (2) Hermann, T. Drugs targeting the ribosome. *Curr. Opin. Struct. Biol.* **2005**, *15*, 355–366.
- (3) Hermann, T.; Tor, Y. RNA as a target for small-molecule therapeutics. *Expert Opin. Ther. Pat.* **2005**, *15*, 49–62.
- (4) Sucheck, S. J.; Wong, C. H. RNA as a target for small molecules. *Curr. Opin. Chem. Biol.* **2000**, *4*, 678–686.
- (5) Nierhaus, K. H.; Wilson, D. N. *Protein Synthesis and Ribosome Structure. Translating the Genome*; Wiley-VCH: Weinheim, Germany, 2004.
- (6) Bannwarth, S.; Gatignol, A. HIV-1 TAR RNA: the target of molecular interactions between the virus and its host. *Curr. HIV Res.* **2005**, *3*, 61–71.
- (7) Ming, Y. Discoveries of Tat-TAR interaction inhibitors for HIV-1. *Curr. Drug Targets-Infect. Disord.* **2005**, *5*, 433–444.
- (8) Robertson, M. P.; Igel, H.; Baertsch, R.; Haussler, D.; Ares, M., Jr.; Scott, W. G. The structure of a rigorously conserved RNA element within the SARS virus genome. *PLoS Biol.* **2005**, *3*, e5.
- (9) Hermann, T. Strategies for the Design of Drugs Targeting RNA and RNA-Protein Complexes. *Angew. Chem., Int. Ed. Engl.* **2000**, *39*, 1890–1904.
- (10) Cheng, A. C.; Calabro, V.; Frankel, A. D. Design of RNA-binding proteins and ligands. *Curr. Opin. Struct. Biol.* **2001**, *11*, 478–484.
- (11) Hofstadler, S. A.; Sannes-Lowery, K. A.; Crooke, S. T.; Ecker, D. J.; Sasmor, H.; Manalili, S.; Griffey, R. H. Multiplexed screening of neutral mass-tagged RNA targets against ligand libraries with elec-



- trospray ionization FTICR MS: a paradigm for high-throughput affinity screening. *Anal. Chem.* **1999**, *71*, 3436–3440.
- (12) Griffey, R. H.; Hofstadler, S. A.; Sannes-Lowery, K. A.; Ecker, D. J.; Crooke, S. T. Determinants of aminoglycoside-binding specificity for rRNA by using mass spectrometry. *Proc. Natl. Acad. Sci. U.S.A.* **1999**, *96*, 10129–10133.
- (13) Hamasaki, K.; Rando, R. R. A high-throughput fluorescence screen to monitor the specific binding of antagonists to RNA targets. *Anal. Biochem.* **1998**, *261*, 183–190.
- (14) Shoichet, B. K. Virtual screening of chemical libraries. *Nature* **2004**, *432*, 862–865.
- (15) Filikov, A. V.; Mohan, V.; Vickers, T. A.; Griffey, R. H.; Cook, P. D.; Abagyan, R. A.; James, T. L. Identification of ligands for RNA targets via structure-based virtual screening: HIV-1 TAR. *J. Comput.-Aided Mol. Des.* **2000**, *14*, 593–610.
- (16) Lind, K. E.; Du, Z.; Fujinaga, K.; Peterlin, B. M.; James, T. L. Structure-Based Computational Database Screening, In Vitro Assay, and NMR Assessment of Compounds that Target TAR RNA. *Chem. Biol.* **2002**, *9*, 185–193.
- (17) Renner, S.; Ludwig, V.; Boden, O.; Scheffer, U.; Gobel, M.; Schneider, G. New inhibitors of the Tat-TAR RNA interaction found with a “fuzzy” pharmacophore model. *Chembiochem.* **2005**, *6*, 1119–1125.
- (18) Gohlke, H.; Klebe, G. Approaches to the Description and Prediction of the Binding Affinity of Small-Molecule Ligands to Macromolecular Receptors. *Angew. Chem., Int. Ed.* **2002**, *41*, 2644–2676.
- (19) Sousa, S. F.; Fernandes, P. A.; Ramos, M. J. Protein-ligand docking: current status and future challenges. *Proteins* **2006**, *65*, 15–26.
- (20) Srinivasan, J.; Leclerc, F.; Xu, W.; Ellington, A. D.; Cedergren, R. A docking and modelling strategy for peptide-RNA complexes: applications to BIV Tat-TAR and HIV Rev-RBE. *Fold Des.* **1996**, *1*, 463–472.
- (21) Leclerc, F.; Cedergren, R. Modeling RNA-ligand interactions: the Rev-binding element RNA-aminoglycoside complex. *J. Med. Chem.* **1998**, *41*, 175–182.
- (22) Hermann, T.; Westhof, E. Docking of cationic antibiotics to negatively charged pockets in RNA folds. *J. Med. Chem.* **1999**, *42*, 1250–1261.
- (23) Mu, Y.; Stock, G. Conformational dynamics of RNA-peptide binding: a molecular dynamics simulation study. *Biophys. J.* **2006**, *90*, 391–399.
- (24) Chen, Q.; Shafer, R. H.; Kuntz, I. D. Structure-based discovery of ligands targeted to the RNA double helix. *Biochemistry* **1997**, *36*, 11402–11407.
- (25) Kang, X.; Shafer, R. H.; Kuntz, I. D. Calculation of ligand-nucleic acid binding free energies with the generalized-born model in DOCK. *Biopolymers* **2004**, *73*, 192–204.
- (26) Leclerc, F.; Karplus, M. MCSS-based predictions of RNA binding sites. *Theor. Chem. Acc.* **1999**, *101*, 131–137.
- (27) Detering, C.; Varani, G. Validation of automated docking programs for docking and database screening against RNA drug targets. *J. Med. Chem.* **2004**, *47*, 4188–4201.
- (28) Morley, S. D.; Afshar, M. Validation of an empirical RNA-ligand scoring function for fast flexible docking using Ribodock. *J. Comput.-Aided Mol. Des.* **2004**, *18*, 189–208.
- (29) Gohlke, H.; Klebe, G. Statistical potentials and scoring functions applied to protein-ligand binding. *Curr. Opin. Struct. Biol.* **2001**, *11*, 231–235.
- (30) Jiang, L.; Gao, Y.; Mao, F.; Liu, Z.; Lai, L. Potential of mean force for protein-protein interaction studies. *Proteins* **2002**, *46*, 190–196.
- (31) Zhang, C.; Liu, S.; Zhu, Q.; Zhou, Y. A knowledge-based energy function for protein-ligand, protein-protein, and protein-DNA complexes. *J. Med. Chem.* **2005**, *48*, 2325–2335.
- (32) Muegge, I.; Martin, Y. C. A general and fast scoring function for protein-ligand interactions: A simplified potential approach. *J. Med. Chem.* **1999**, *42*, 791–804.
- (33) Mitchell, J. B. O.; Laskowski, R. A.; Alex, A.; Thornton, J. M.; BLEEP-potential of mean force describing protein-ligand interactions: I. Generating potential. *J. Comput. Chem.* **1999**, *20*, 1165–1176.
- (34) Gohlke, H.; Hendlich, M.; Klebe, G. Knowledge-based Scoring Function to Predict Protein-Ligand Interactions. *J. Mol. Biol.* **2000**, *295*, 337–356.
- (35) Yang, C. Y.; Wang, R.; Wang, S. M-score: a knowledge-based potential scoring function accounting for protein atom mobility. *J. Med. Chem.* **2006**, *49*, 5903–5911.
- (36) Muegge, I. PMF scoring revisited. *J. Med. Chem.* **2006**, *49*, 5895–5902.
- (37) Muryshev, A. E.; Tarasov, D. N.; Butygin, A. V.; Butygina, O. Y.; Aleksandrov, A. B.; Nikitin, S. M. A novel scoring function for molecular docking. *J. Comput.-Aided Mol. Des.* **2003**, *17*, 597–605.
- (38) Ozrin, V. D.; Subbotin, M. V.; Nikitin, S. M. PLASS: protein-ligand affinity statistical score—a knowledge-based force-field model of interaction derived from the PDB. *J. Comput.-Aided Mol. Des.* **2004**, *18*, 261–270.
- (39) Gohlke, H.; Hendlich, M.; Klebe, G. Predicting Binding Modes, Binding Affinities and “Hot Spots” for Protein-Ligand Complexes using a Knowledge-based Scoring Function. *Perspect. Drug Discovery Des.* **2000**, *20*, 115–144.
- (40) Sotriffer, C. A.; Gohlke, H.; Klebe, G. Docking into knowledge-based potential fields: A comparative evaluation of DrugScore. *J. Med. Chem.* **2002**, *45*, 1967–1970.
- (41) Velec, H. F.; Gohlke, H.; Klebe, G. DrugScore(CSD)-knowledge-based scoring function derived from small molecule crystal data with superior recognition rate of near-native ligand poses and better affinity prediction. *J. Med. Chem.* **2005**, *48*, 6296–6303.
- (42) Sippl, M. J. Calculation of conformational ensembles from potentials of mean force. An approach to the knowledge-based prediction of local structures in globular proteins. *J. Mol. Biol.* **1990**, *213*, 859–883.
- (43) Zhang, C.; Liu, S.; Zhou, H.; Zhou, Y. An accurate, residue-level, pair potential of mean force for folding and binding based on the distance-scaled, ideal-gas reference state. *Protein Sci.* **2004**, *13*, 400–411.
- (44) Ruvinisky, A. M.; Kozintsev, A. V. The key role of atom types, reference states, and interaction cutoff radii in the knowledge-based method: new variational approach. *Proteins* **2005**, *58*, 845–851.
- (45) SYBYL Molecular Modeling Software, 7.3; Tripos Inc.: St. Louis, MO, 2006.
- (46) Morris, G. M.; Goossell, D. S.; Huey, R.; Hart, W. E.; Belew, R. K.; Olson, A. J. Automated docking using a Lamarckian genetic algorithm and an empirical binding free energy function. *J. Comput. Chem.* **1998**, *19*, 1693–1662.
- (47) Radestock, S.; Bohm, M.; Gohlke, H. Improving binding mode predictions by docking into protein-specifically adapted potential fields. *J. Med. Chem.* **2005**, *48*, 5466–79.
- (48) Moitessier, N.; Westhof, E.; Hanessian, S. Docking of aminoglycosides to hydrated and flexible RNA. *J. Med. Chem.* **2006**, *49*, 1023–1033.
- (49) Cornell, W. D.; Cieplak, C. I.; Bayly, I. R.; Gould, I. R.; Merz, K. M.; Ferguson, D. M.; Spellmeyer, D. C.; Fox, T.; Caldwell, J. W.; Kollman, P. A. A second generation force field for the simulation of proteins, nucleic acids, and organic molecules. *J. Am. Chem. Soc.* **1995**, *117*, 5179–5197.
- (50) Gasteiger, J.; Marsili, M. Iterative Partial Equalization of Orbital Electronegativity-A rapid Access to Atomic Charges. *Tetrahedron* **1980**, *36*, 3219–3228.
- (51) Case, D. A.; Cheatham, T. E., III; Darden, T.; Gohlke, H.; Luo, R.; Merz, K. M., Jr.; Onufriev, A.; Simmerling, C.; Wang, B.; Woods, R. J. The Amber biomolecular simulation programs. *J. Comput. Chem.* **2005**, *26*, 1668–1688.
- (52) Zhang, C.; Liu, S.; Zhou, H.; Zhou, Y. The dependence of all-atom statistical potentials on structural training database. *Biophys. J.* **2004**, *86*, 3349–3358.
- (53) Ferrara, P.; Gohlke, H.; Price, D. J.; Klebe, G.; Brooks, C. L. Assessing scoring functions for protein-ligand interactions. *J. Med. Chem.* **2004**, *47*, 3032–3047.
- (54) Zimmermann, G. R.; Jenison, R. D.; Wick, C. L.; Simorre, J. P.; Pardi, A. Interlocking structural motifs mediate molecular discrimination by a theophylline-binding RNA. *Nat. Struct. Biol.* **1997**, *4*, 644–649.
- (55) Hermann, T.; Patel, D. J. Adaptive recognition by nucleic acid aptamers. *Science* **2000**, *287*, 820–5.
- (56) Yoshizawa, S.; Fourmy, D.; Puglisi, J. D. Structural origins of gentamicin antibiotic action. *EMBO J.* **1998**, *17*, 6437–6448.
- (57) Perola, E.; Walters, W. P.; Charifson, P. S. A detailed comparison of current docking and scoring methods on systems of pharmaceutical relevance. *Proteins* **2004**, *56*, 235–249.
- (58) Wang, R.; Lu, Y.; Wang, S. Comparative evaluation of 11 scoring functions for molecular docking. *J. Med. Chem.* **2003**, *46*, 2287–2303.
- (59) Tsai, C.-J.; Kumar, S.; Ma, B.; Nussinov, R. Folding funnels, binding funnels, and protein function. *Protein Sci.* **1999**, *8*, 1181–1190.
- (60) Wang, J.; Verkhrivker, G. M. Energy landscape theory, funnels, specificity, and optimal criterion of biomolecular binding. *Phys. Rev. Lett.* **2003**, *90*, 188101.
- (61) Verkhrivker, G. M.; Bouzida, D.; Gehlhaar, D. K.; Rejto, P. A.; Freer, S. T.; Rose, P. W. Complexity and simplicity of ligand-macromolecule interactions: the energy landscape perspective. *Curr. Opin. Struct. Biol.* **2002**, *12*, 197–203.
- (62) Press, W. H.; Teukolsky, S. A.; Vetterling, W. T.; Flannery, B. P. In *Numerical Recipes in Fortran 77: The Art of Scientific Computing*, 2nd ed.; Cambridge University Press: New York, NY, 2001; pp 633–639.